Journal of Electronic Materials, Vol. 27, No. 3, 1998

The Microstructures of the Sn-Zn-Al Solder Alloys

KWANG-LUNG LIN, LI-HSIANG WEN, and TZY-PIN LIU

Department of Materials Science and Engineering, National Cheng Kung University, Tainan, Taiwan 701, Republic of China

The microstructures of the Sn-Zn-Al lead-free solders have been investigated using scanning electron microscopy. The Al and Zn contents of the solders investigated were 0.45%~4.5% and 8.55%~85.5%, respectively. The solders were prepared from the Zn-5Al master alloy and Sn. The precipitates formed in these solders were analyzed for their compositions with energy dispersive spectroscopy. The eutectic temperature and the transition temperatures of these solders upon cooling were identified with cooling curves as well as with differential scanning calorimetry.

Key words: Cooling curve, differential scanning calorimetry, lead-free solder, microstructure

INTRODUCTION

The development of Pb-free solders has become an important issue for electronic interconnection materials because of the health and environmental safety concerning lead usage. Binary Pb-free solder systems that have been disclosed in the literature include Sn-Ag, Sn-Au, Sn-Bi, Sn-Cd, Sn-Sb, and Sn-Zn.[1–8] The Pb-free solder systems discussed also include certain ternary systems like Sn-Ag-Zn,[9] Sn-Zn-In,[10,11] Sn-Ag-Sb,[12] Bi-Sb-Sn,[13] Sn-Bi-Ag,[14] and Sn-Ag-Cu.[15] The addition of Zn in the Sn-Ag-Zn[10,11] system improves the mechanical strength of the Sn-3.5%Ag solder.

The 91Sn-9Zn is the eutectic composition of the Sn-Zn system with a melting point of 198°C, which is very close to the eutectic temperature, 183°C, of the Sn-Pb system. The Sn-Zn solders have better mechanical strength than the conventional Sn-Pb solders, yet suffering a higher oxidation potential. Al has been incorporated with Zn to enhance the atmospheric corrosion resistance of the conventional galvanizing coatings for steel. Zn-5Al and 55Al-Zn coatings are the most commonly commercialized Al-Zn series of coatings such as GALFAN® and GALVALUME®. A series of studies tried to incorporate Al with the Sn-Zn solders. The addition of Al to the Sn-Zn solder is kept at low levels in order to keep the melting point as low as possible. Al may form solid solutions with Zn and Sn. An equilibrium phase diagram has been reported[16] for this particular ternary system which has a eutectic point at 197°C. The diffusion paths of various Sn-Zn-Al systems have also been discussed[16] at various isotherms. The present work started from Zn-5Al alloy and Sn to prepare and to investigate the thermal behaviors of thus prepared various Pb-free Sn-Zn-Al solders. The oxidation behavior of the Sn-Zn-Al alloys must be investigated to alleviate the concerns on the formation of the oxide slag during soldering. In addition to Al, certain transition metals such as Cr, Ti, and Zr may assist in improving the oxidation resistance or corrosion resistance of the alloys in view of the passivation behaviors of these elements. Nevertheless, these elements have high melting points and are not known to form low melting eutectic alloys with Sn and Zn, and thus are excluded from consideration in this work.

The ternary Sn-Zn-Al system possesses a complicated phase transition behavior based on the equilibrium studies mentioned above.[16] The solders may encounter a solidification sequence during the fabrication of the electronic interconnections, for instance, the wave soldering or solder reflow. A detailed understanding of the solidification behavior as well as the phase formation is of interest as far as the control of the solder joint property is concerned. The currently existing phase diagram,[16] however, can only provide rather limited information for predicting the room temperature phases, not to mention the occurrences during solidification. It is not the interest of this present work to investigate the complete phase equilibria as for establishing the phase diagram of this ternary Sn-Zn-Al system. Instead, this work is a detailed investigation to the solidification behavior of the various compositions of the Sn-Zn-Al solders.

(Received December 30, 1996; accepted August 15, 1997)

EXPERIMENTAL PROCEDURE

The Sn-Zn-Al solders were prepared by melting the Zn-5Al master alloy with Sn. Accordingly, the solder compositions are YSn-X(Zn-5Al) wherein X and Y represent the weight percentage of Zn-5Al and Sn, respectively. Thus, prepared solders were investigated for their cooling curves, thermal behaviors, and microstructures.

The cooling curves were investigated by measuring the temperature variations of molten solders in a Al_2O_3 crucible. The solders were melted at 500°C for 2 h and then cooled slowly in the furnace. A thermocouple for measuring the temperature changes was embedded in the bulk solder. The voltage variations of the thermocouple were read with a multimeter. The voltages were converted to temperature readings and recorded as a cooling curve with a personal computer. The thermocouple has been calibrated with pure Zn and Sn to assure the correct readings of their melting points.

The thermal behaviors of the solders were investigated with differential scanning calorimetry (DSC). A piece of about 10 mg solder was heated in a Pt cell at a heating rate of 10°C/min up to 500°C under a Ar atmosphere. The cooling rate was also 10°C/min. The thermal behaviors of the solders were recorded during heating and cooling in the calorimeter, the cooling behaviors were compared with the results obtained from cooling curves.

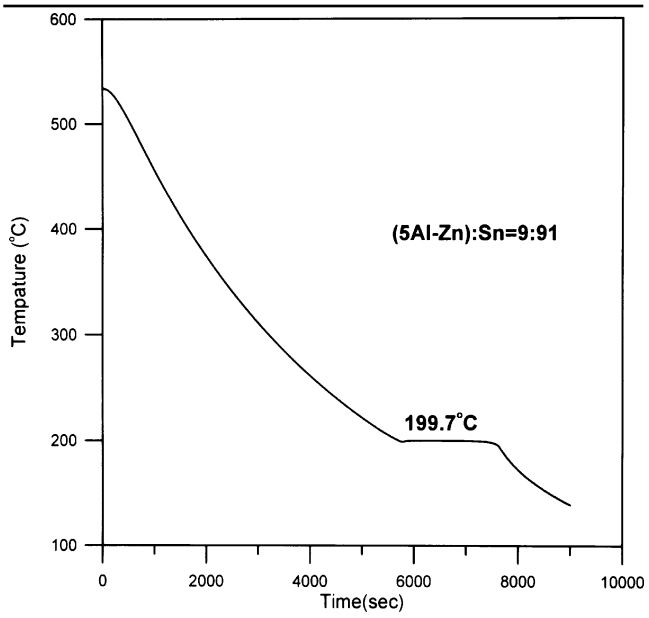

Fig. 1. The cooling curve of the 9(Zn-5Al)-91Sn solder.

For microstructural investigation, as-cast solders were used. It is expected that the cooling rate of the as-cast solders was slower than that of the normally applied solder joint due to the difference in the mass. The degree of deviation in microstructure between each other remains to be explored as these solders have not been practiced for joint application. The microstructures of the as-cast solders were investigated with an optical microscope (OM) and a scanning electron microscope (SEM). The compositions of the precipitates and phases in the solidified solders were analyzed with energy dispersive spectroscopy (EDS).

RESULTS AND DISCUSSION

The solders investigated in this present work were the solders in which the Y:X (weight fractions) ratios of YSn-X(Zn-5Al) ranged from 91:9 to 40:60. The compositions of the prepared solders were 91Sn-8.55Zn-0.45Al (91:9), 80Sn-19Zn-1Al (80:20), 70Sn-28.5Zn-1.5Al (70:30), 60Sn-38Zn-2Al (60:40), 50Sn-47.5Zn-2.5Al (50:50), 57Zn-40Sn-3Al (40:60), 66.5Zn-30Sn-3.5Al (30:70), 76Zn-20Sn-4Al (20:80), and 85.5Zn-10Sn-4.5Al (10:90), with Y:X ratios presented in the parentheses. The results of cooling curve, DSC, and microstructural investigations of each composition are to be discussed below.

91Sn-9(Zn-5Al) Solder

This composition is very close to the eutectic composition of the ternary Sn-Zn-Al system.[16] There exists a plateau region at 199.7°C in the cooling curve of this solder as seen in Fig. 1. No inflection temperature other than 199.7°C was observed in the cooling curve, indicating a typical cooling behavior of a eutectic system. The optical and SEM micrograph of the eutectic microstructure is shown in Fig. 2. It indicates a typical lamella eutectic microstructure. The primarily solidified phase, the dark phase in Fig. 2a, of the

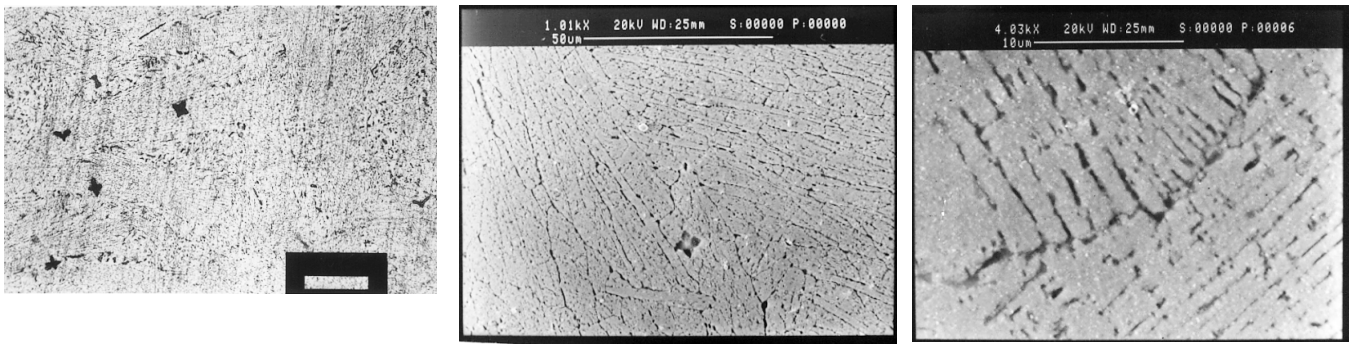

a b c

Fig. 2. The microstructure of the 9(Zn-5Al)-91 Sn solder, (a) optical micrograph, (b) SEM micrograph, and (c) SEM micrograph of the eutectic microstructure.

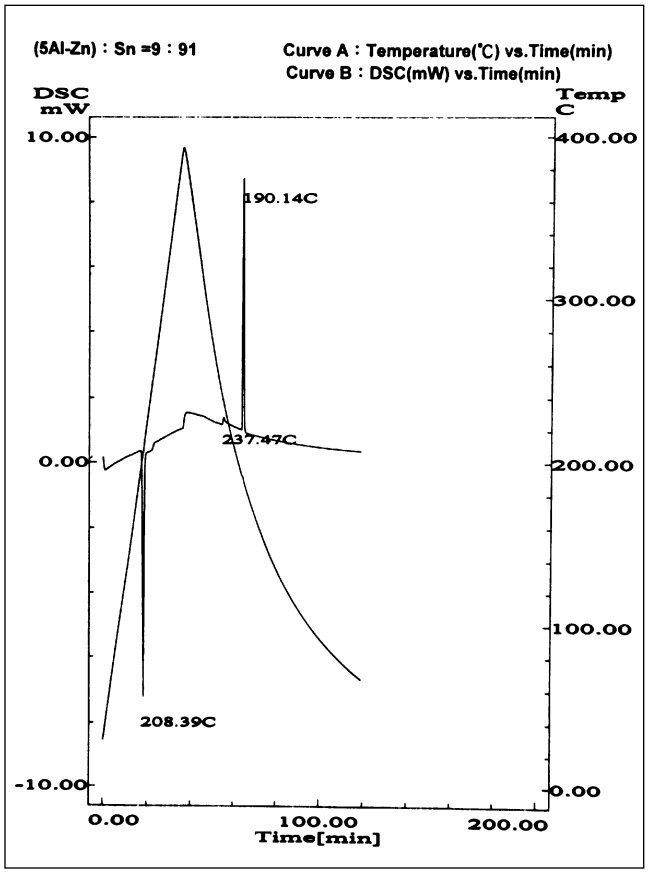

Fig. 3. The DSC curve of the 91Sn-9(Zn-5Al) solder.

eutectic structure was analyzed and consists of (83.7~90.5)Sn-(5.41~12.04)Al-(3.19~5.77)Zn, while the composition of the secondarily solidified phase, the white phase of Fig. 2a, was 98.3Sn-1.36Zn-0.33Al. This is reasonable as the phase with greater contents of Al and Zn is expected to solidify first. The optical micrograph of 91Sn-9(Zn-5Al) shows "star" precipitates distributed in the eutectic phase, Fig. 2b. The composition, analyzed with EDS, of this "star" precipitate, Fig. 2c, is 39.2Zn-35.1Al-25.7Sn, corresponding to a stoichiometry of Al_6Zn_3Sn. The high Al and Zn contents of this precipitate is indicative that it precipitates prior to the eutectic reaction. The DSC curve, Fig. 3, of this 91Sn-9(Zn-5Al) solder indicates a peak upon heating while two peaks upon cooling. A comparison between the DSC curve, Fig. 3, and the cooling curve, Fig. 1, indicates that the heating and cooling rates, 10°C/min, of the DSC experiments are so fast that an undercooling or superheating occurred. A significant undercooling was also reported for 63Sn-37Pb solder when investigated with DSC.[17] A plateau eutectic temperature at 199.7°C was detected with the cooling curve at a cooling rate of 3°C/min, Fig. 1, while about a 9°C difference from this eutectic temperature was achieved with DSC investigation for both heating (208.4 vs 199.7°C) and cooling (190.1 vs 199.7°C). In other words, the peak temperatures observed in DSC curve may be regarded as 9°C above (upon heating) or below (upon cooling) the actual

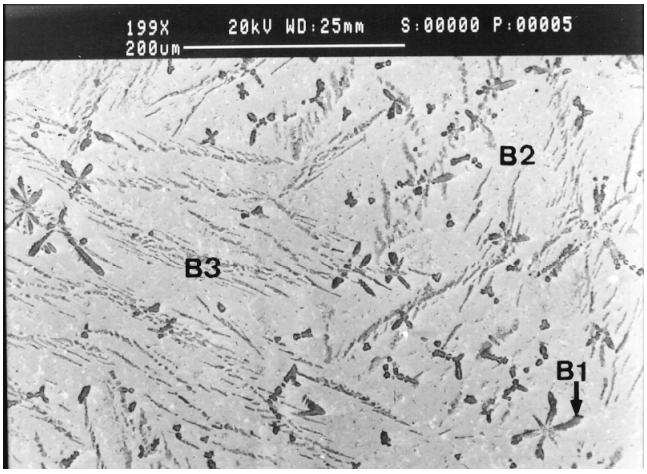

Fig. 4. The cooling curve of the 80Sn-20(Zn-5Al) solder.

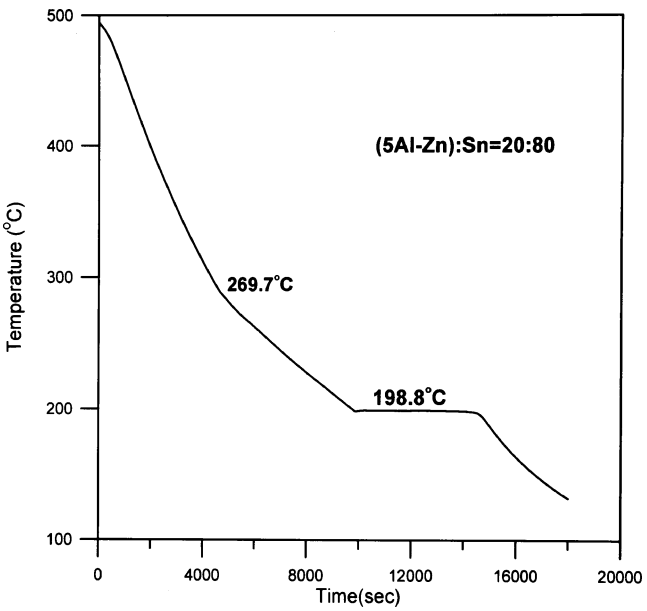

Fig. 5. The DSC curve of the 80Sn-20(Zn-5Al) solder.

temperature.

The tiny peak occurring upon cooling at 237.5°C on the DSC analysis, which must be 246.5°C according to the above discussion, is ascribed to the "star" precipitate, analyzed to be Al_6Zn_3Sn, observed in Fig. 2a and 2b. The quantity of this precipitate counts for only a very limited volume fraction as seen in the micrographs and thus a relatively small DSC peak is observed. In addition, this Al_6Zn_3Sn precipitate is expected to have a phase transition temperature higher than the eutectic temperature in view of its high Al and Zn contents in comparing to that of the eutectic phase.

80Sn-20(Zn-5Al) Solder

The SEM micrograph, Fig. 4, of the 80Sn-20(Zn-5Al) solder shows a precipitate, B1, and a primary phase, B3, in addition to the continuous matrix B2. The continuous phase, B2, was analyzed to have a composition of 98.7Sn-0.71Al-0.56Zn. The composi-

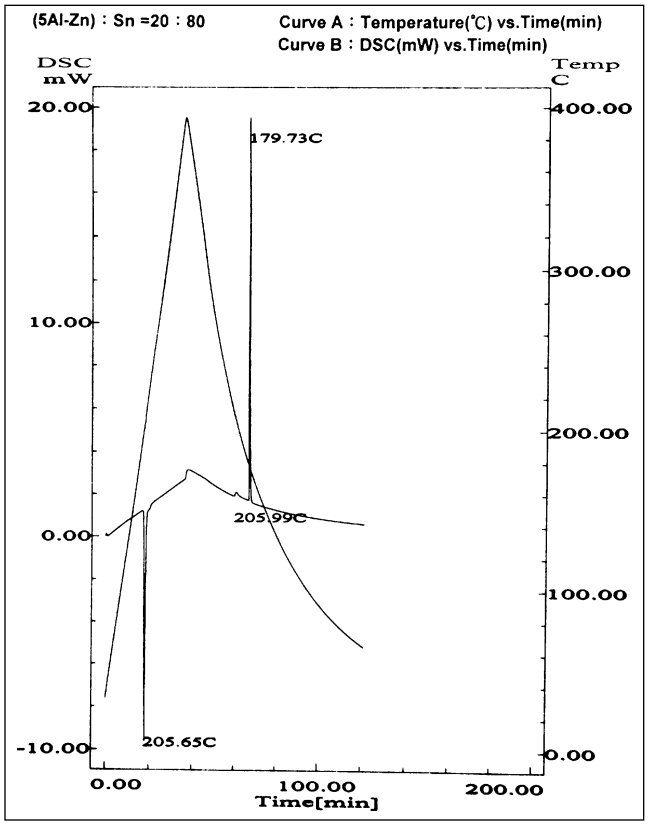

Fig. 6. The SEM micrograph of the 80Sn-20(Zn-5Al) solder.

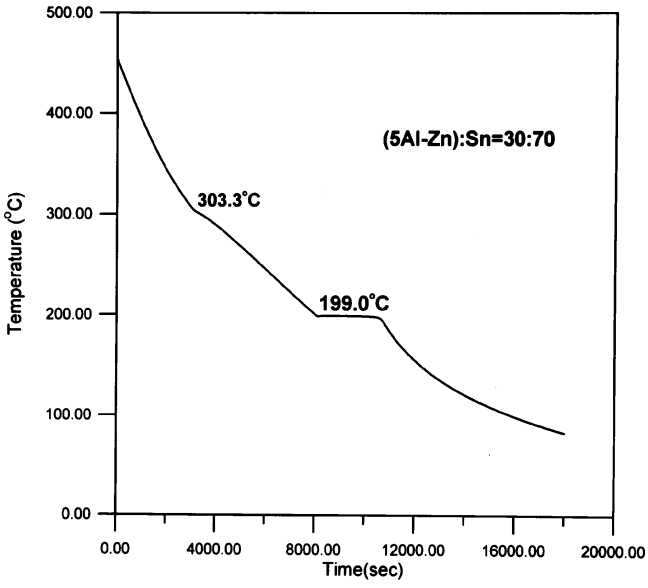

Fig. 7. The cooling curve of the 70Sn-30(Zn-5Al) solder.

tions of B1 and B3 were found to be 58.8Al-36.2Zn-5.02Sn and 64.4Zn-30.0Sn-5.63Al, respectively, which have greater contents of Al and Zn than that of the Al_6Zn_3Sn precipitate observed in the 91Sn-9(Zn-5Al) solder as detected in Fig. 2. Thus, the transition temperatures of the B1 and B3 phases are expected to be greater than that, 237.5°C, of the Al_6Zn_3Sn precipitate as seen in the following.

The cooling curve, Fig. 5, of this composition of solder reveals a high temperature inflection at around

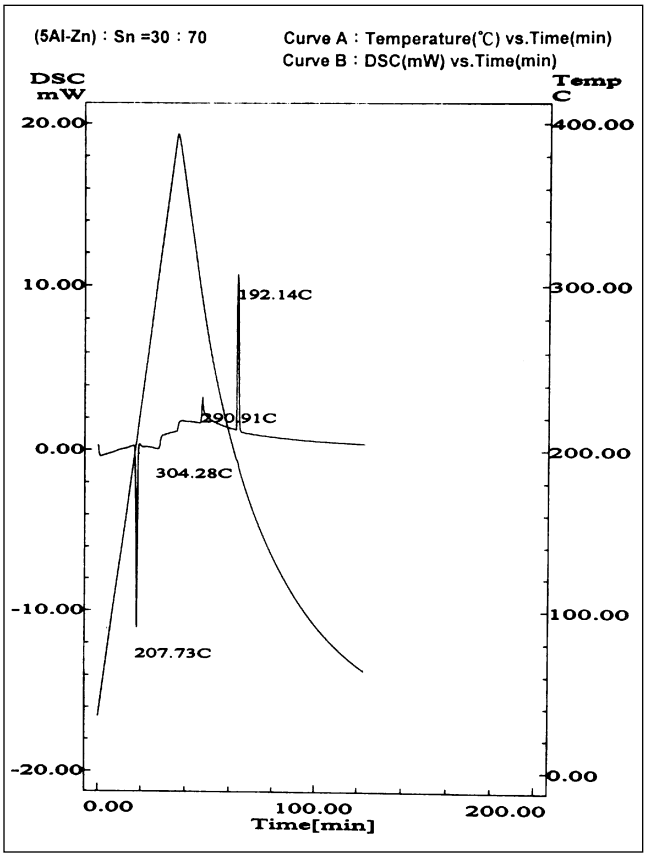

Fig. 8. The DSC curve of the 70Sn-30(Zn-5Al) solder.

269.7°C, in addition to the plateau temperature 198.8°C. During cooling, peaks at around 206 and 180°C were detected with DSC, Fig. 6. A very slight inflection behavior is also detected at around 290°C on the DSC curve. The DSC peaks at 180 and 206°C appear to correspond with the transition temperatures of 198.8 and 269.7°C on the cooling curves. The deviations in the temperature are ascribed to the undercooling behavior. The extent of undercooling may depend on the investigated materials as well as on the wetting between the material and the DSC cell.[17] In view of the compositions of the various phases in this solder, the transition temperatures of the B2 and B3 phases are assayed to be 198.8 and 269.7°C, respectively. The B1 phase consists of high contents of the high melting temperature elements Al (78.5%) and Zn (20.0%). Accordingly, it is reasonable to assume a transition temperature of no less than 290°C for the B1 phase. This transition is not observable on the cooling curve as the B1 phase counts for only a small volume fraction.

70Sn-30(Zn-5Al) Solder

The solidification of the continuous phase at 199°C is still observed for this composition in the cooling curve shown in Fig. 7, which is 192.1°C on the DSC curve. A kink in the cooling curve exists at 303.3°C. This deflection point corresponds with the DSC peak at 290.9°C as detected during the cooling investigation, Fig. 8. Accordingly, only a primary phase would

be expected to form prior to the solidification of the continuous phase.

The compositions of the zinc primary phases observed in SEM micrographs Figs. 9a and 9b, are 65.7Zn-20.7Al-13.6Sn for C1, 80.9Zn-15.4Sn -3.78Al for C2, and 75.3Zn-13.8Sn-10.8Al for C3. These primary phases form a dendritic microstructure as seen in Fig. 9a. The Al contents of this Zn dominant phase vary from 3.8 to 20.7%, while the Sn content remains relatively constant. The composition of the continuous phase is 98.1Sn-1.36Zn-0.532Al. Sn exhibits a restricted solid solubility in Zn, as low as 0.05~0.1wt% at the eutectic temperature.[18] The solubility in each other for Al and Sn are also very restricted.[18] Accordingly, the high Sn contents of these analyses are suspected to be an error due to the interference from the continuous matrix phase. For instance, the C2 structure of Fig. 9b shows a mixture of the pale continuous phase and the dark primary phase. It is thus concluded that the primary phase(s) is (are) mainly the Al-in-Zn solid solution(s).

60Sn-40(Zn-5Al) Solder

The microstructure of the 60Sn-40(Zn-5Al) solder, Figs. 10a and 10b, is similar to that of the 70Sn-30(Zn-5Al) solder, Fig. 9a, except that there are more fractions of the primary phases. In addition, the compositions of the primary phases indicate the formation of an aluminum phase, D1 in Fig. 10b, and a zinc phase, D2. The compositions of these phases are 52.0Al-39.7Zn-8.30Sn for D1 and 90.9Zn-6.71Al-2.43Sn for D2. The composition of the continuous phase was found to be 95.3 Sn-4.26Zn-0.42Al.

Both results of cooling curve, Fig. 11, and DSC, Fig. 12, show two distinct transitions at the temperatures greater than eutectic temperature. In this particular experiment, undercooling is also detected with DSC. The transition temperatures of these phases are assigned to be 325°C (313°C) for D1, 269.9°C (265.5°C) for D2, and 197.6°C(190.3°C) for D3. The temperatures in the parentheses are obtained from the DSC curve.

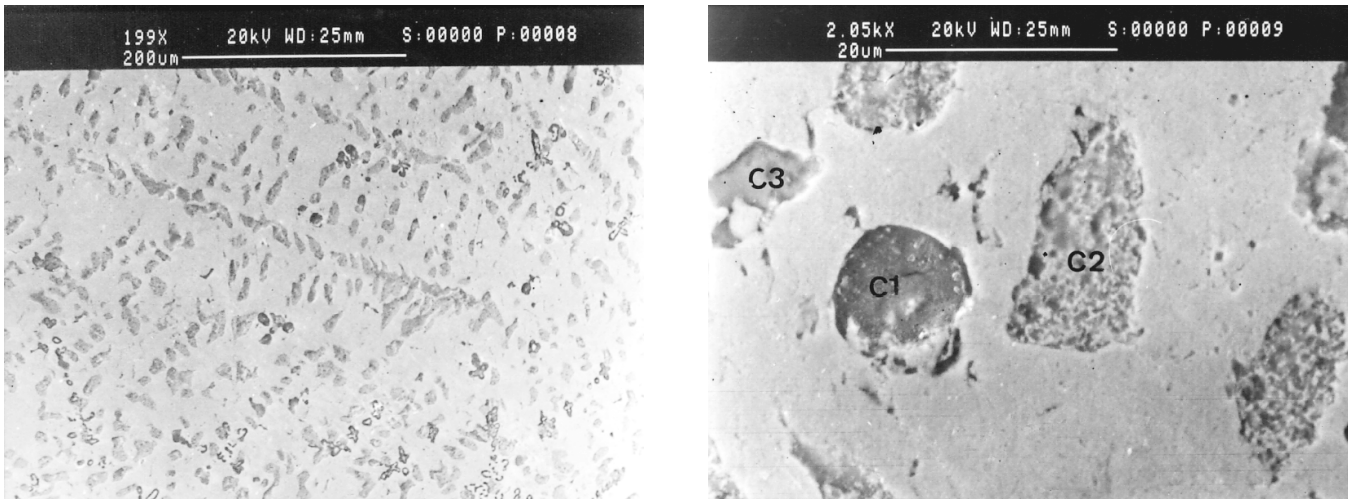

a b

Fig. 9. (a) The SEM micrograph of the 70Sn-30(Zn-5Al) solder, and (b) the inset of (a).

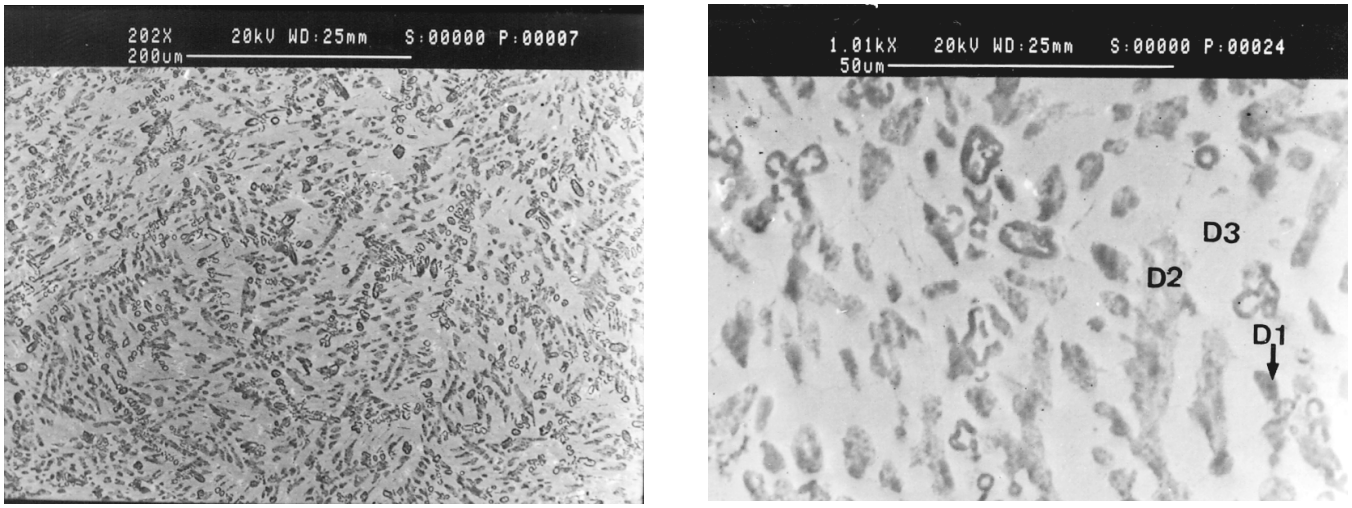

a b

Fig. 10. (a) The SEM micrograph of the 60Sn-40(Zn-5Al) solder, and (b) a higher magnification of (a).

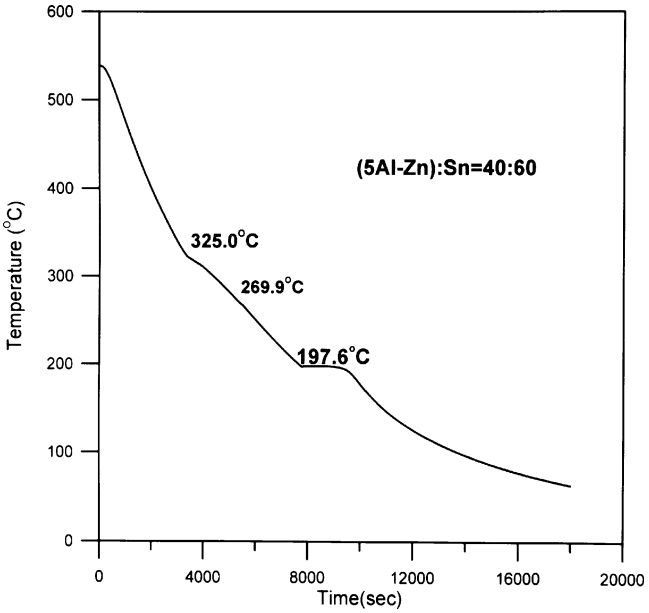

Fig. 11. The cooling curve of the 60Sn-40(Zn-5Al) solder.

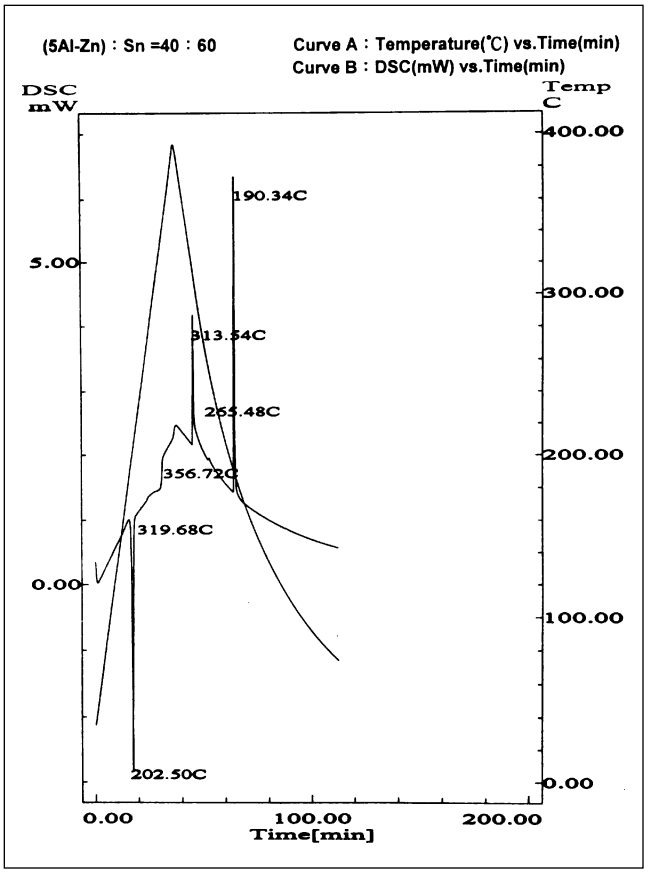

Fig. 12. The DSC curve of the 60Sn-40(Zn-5Al) solder.

50Sn-50(Zn-5Al) Solder

The DSC curve, Fig. 13, shows two distinct transitions occuring at temperatures greater than 300, 324.8, and 335.4°C. A small transition peak is also found visible at between 300 and 295°C. The continuous phase solidifies at 191.3°C. The cooling curve

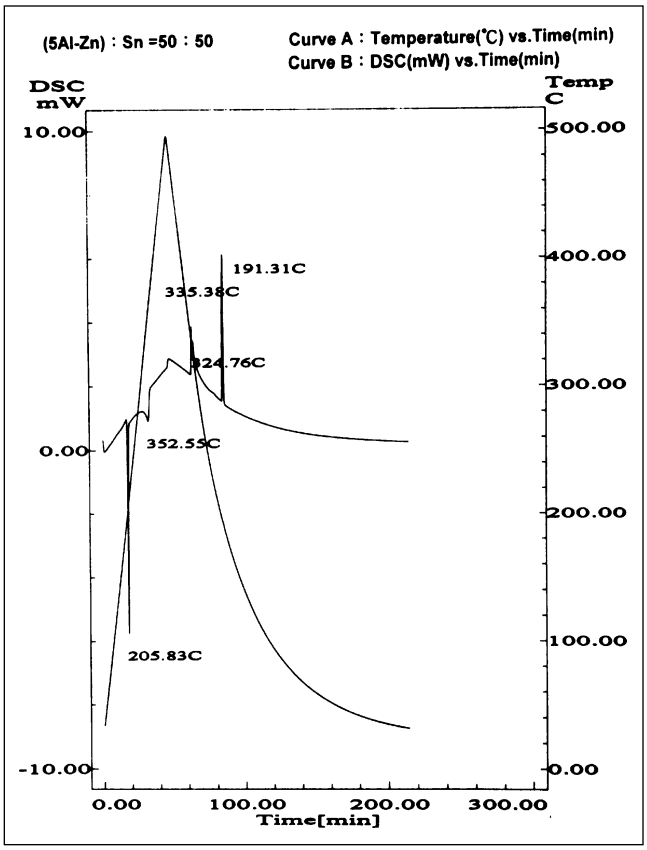

Fig. 13. The DSC curve of the 50(Zn-5Al)-50Sn solder.

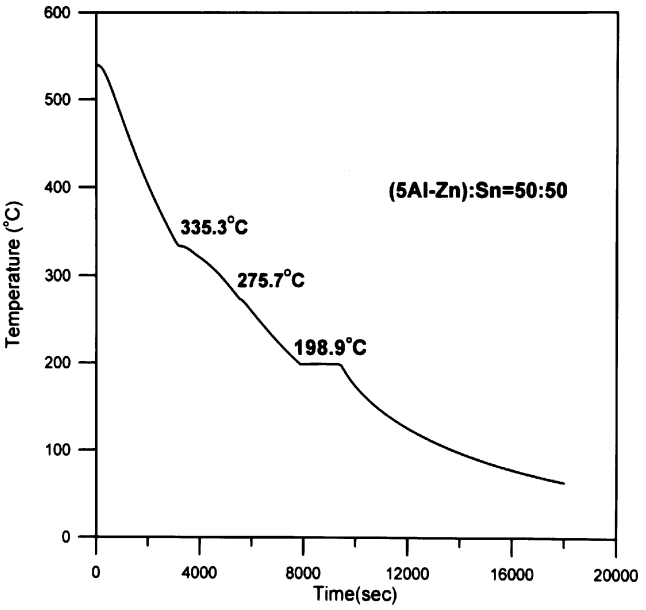

Fig. 14. The cooling curve of the 50(Zn-5Al)-50Sn solder.

investigations, Fig. 14, show three distinct transition temperatures at 335.3, 275.7, and 198.9°C. A shoulder exists in the cooling curve immediately below 335.3°C. On the basis of the DSC and cooling curve results, it is believed that there are four transitions, although only three phases are identifiable through the EDS composition analysis. Three distinct phases, including the continuous phase which must be the

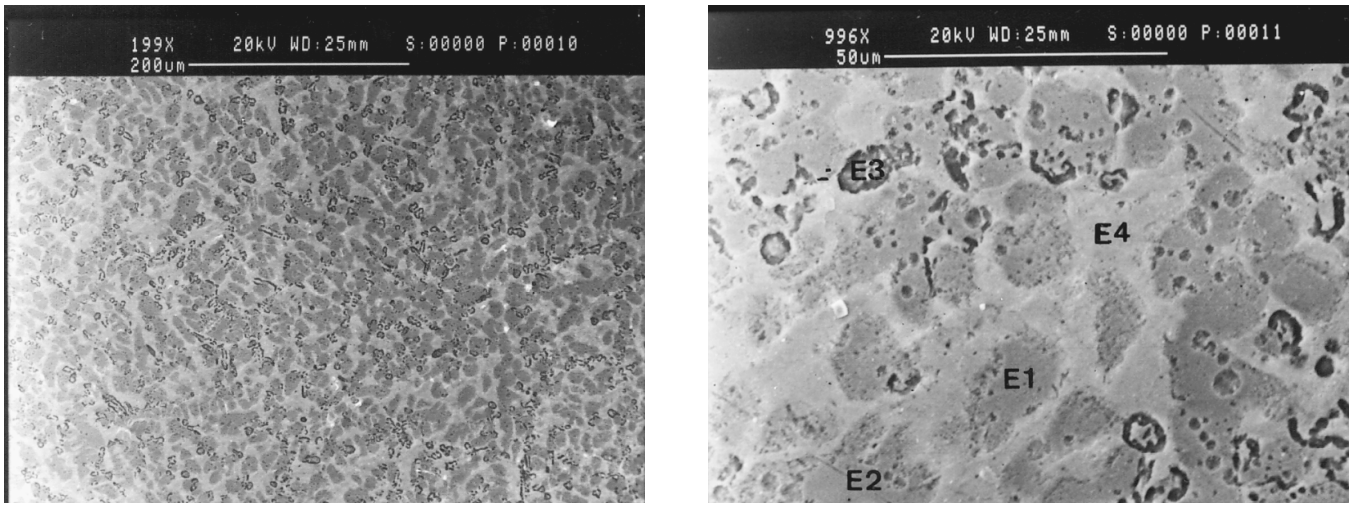

a b

Fig. 15. (a) The SEM micrograph of the 50(Zn-5Al)-50Sn solder, and (b) a higher magnification of (b).

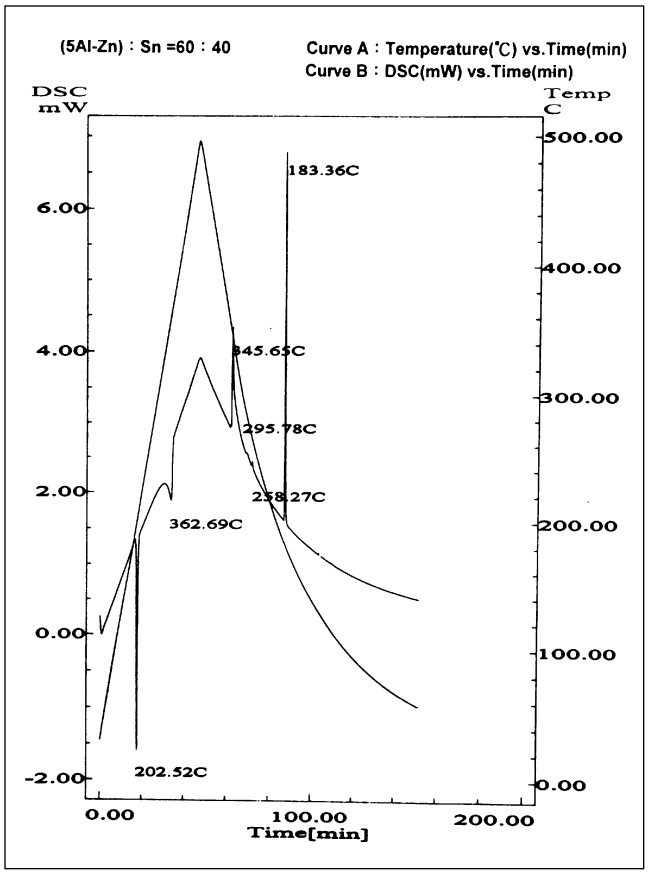

Fig. 16. The DSC curve of the 60(Zn-5Al)-40Sn solder.

eutectic phase according to the transition temperature, are found in the SEM micrograph, Figs. 15a and 15b. The compositions of these phases are (97.3~95.4)Zn-(1.94~3.21)Al-(0.78~1.37)Sn for E1 and E2, (36.4~38.6)Al-(35.6~38.3)Sn-(23.2~28.0)Zn for E3 and E5, and 95.4Sn-3.80Zn-0.83Al for E4. The solder thus consists of a dendritic zinc phase and a high Al content phase, in addition to the continuous eutectic matrix.

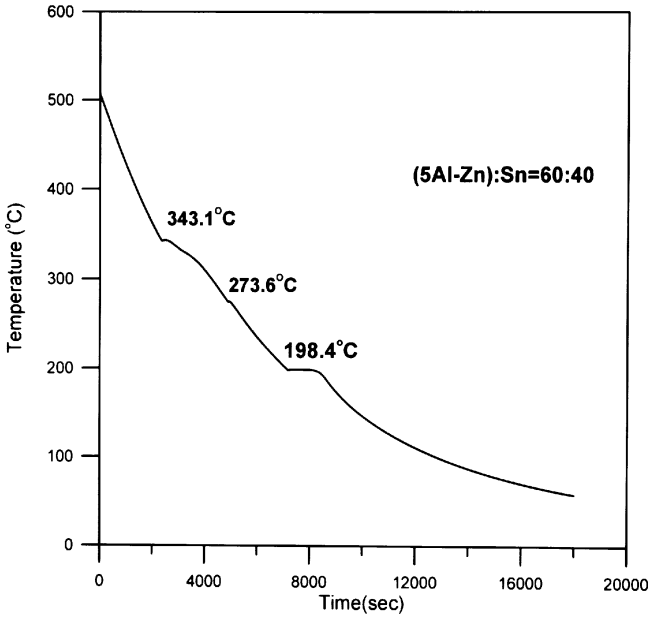

Fig. 17. The cooling curve of the 60(Zn-5Al)-40Sn solder.

60(Zn-5Al)-40Sn Solder

Four transition temperatures are visible in the DSC investigation, Fig. 16, and these are 345.7, 295.8, 258.3, and 183.4°C. The cooling curve behavior (Fig. 17) of this solder is very similar to that (Fig. 14) of the 50Sn-50(Zn-5Al) solder, although there are mainly three phases observed in the microstructure, Fig. 18. The high Al content precipitates, F1, precipitating primarily in the continuous matrix, consists of 53.6Al-24.0Sn-22.4Zn. The continuous phase, F2, which solidifies last has a composition of 94.6Sn-4.56Zn-0.84Al. The dendritic phase is also a zinc phase, F3, with a composition of (97.1~99.5)Zn-(1.59~1.91)Al-1.00Sn. The cooling curve of this solder exhibits a plateau region at 198.4°C, and two deflections on the cooling curve at 343.1 and 273.6°C. The phases and microstructures of this solder are of the

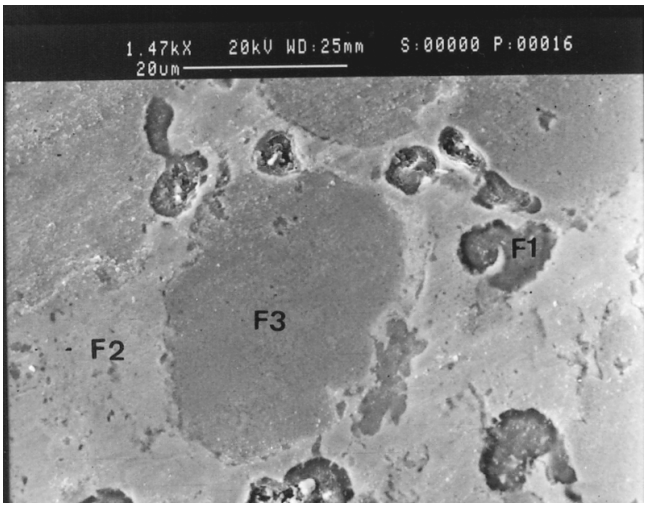

Fig. 18. The SEM micrograph of the 60(Zn-5Al)-40Sn solder.

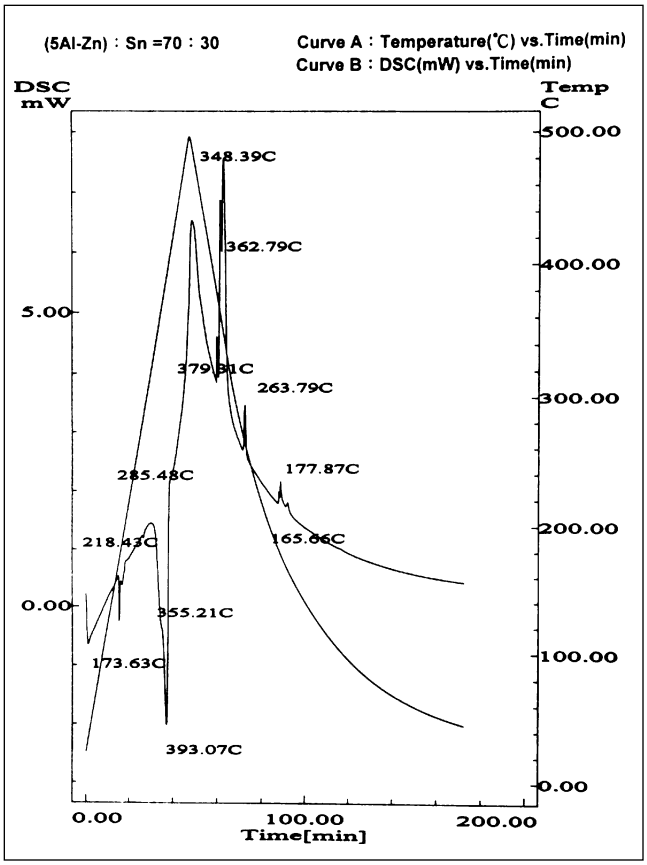

Fig. 19. The DSC curve of the 70(Zn-5Al)-30Sn solder.

same as that of the 50Sn-50(Zn-5Al) solder.

70~90(Zn-5Al)-30~10Sn Solders

The DSC curves of these solders show at least five transitions when the Sn contents are no greater than 30%. Figure 19 shows the DSC curve of the 70(Zn-5Al)-30Sn solder. Six transition peaks are observed upon cooling. The cooling curve, Fig. 20, of the 70(Zn-5Al)-30Sn solder becomes too complicated to identify the transition temperatures, due to the close proximity of these transitions to each other. It is difficult to

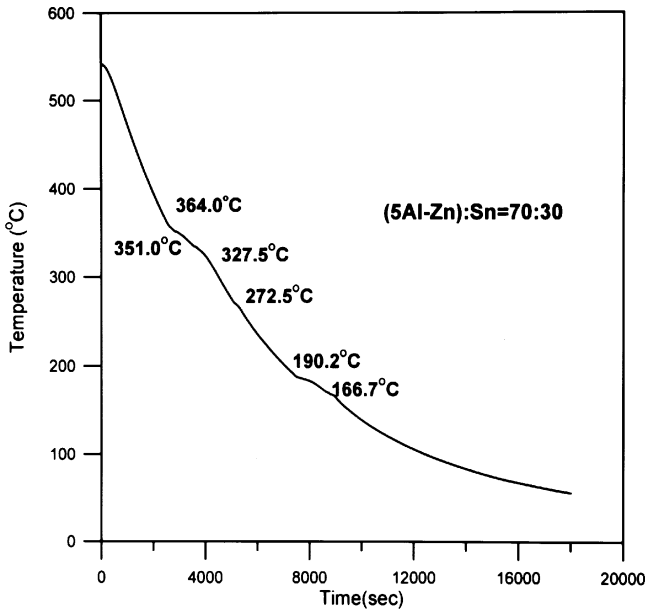

Fig. 20. The cooling curve of the 70(Zn-5Al)-30Sn solder.

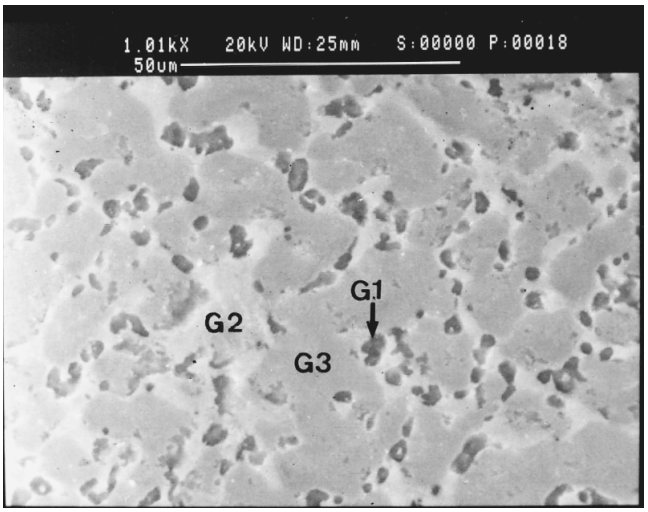

Fig. 21. The SEM micrograph of the 70(Zn-5Al)-30Sn solder.

identify the phases on the SEM micrograph, Fig. 21. Three visually identifiable phases are marked in Fig. 21. The compositions of these three phases are 72.0Al-20.8Zn-7.16Sn, 83.1Sn-15.7Zn-1.21Al, and 94.2Zn-4.21Al-1.58Sn, for G1, G2, and G3, respectively.

The transition peaks, in °C, detected from DSC curves for the solders with 20%Sn and 10%Sn are 351.1, 334.8, 267.4, 176.7, and 167.5 for 80(Zn-5Al)-20Sn, and 382.2, 364.2, 353.3, 263.9, 173.1, and 169.5 for 90(Zn-5Al)-10Sn. The phases identified as shown in Fig. 22 for the 80(Zn-5Al)-20Sn are 77.6Al-17.8Zn-4.56Sn, 86.7Sn-9.36Zn-3.94Al, and 94.6Sn-5.32Al-0.11Sn for H1, H2, and H3 phases, respectively. Meanwhile, the phases in Fig. 23 for the 90(Zn-5Al)-10Sn are identified as 84.7Sn-14.0Zn-1.29Al, 96.5Zn-3.58Al, and 65.7Al-33.0Zn-1.32Sn, for I1, I2, and I3, respectively. Al contents of the higher Zn-containing alloy as described in this section are similar to that of the commonly used die casting alloys. Yet, the Sn

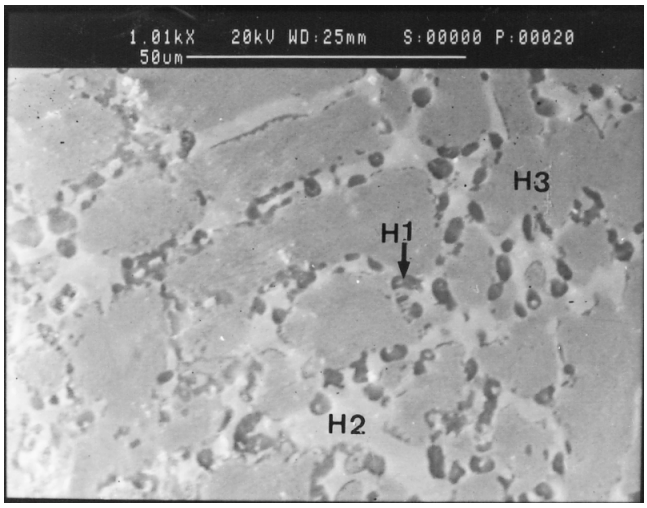

Fig. 22. The SEM micrograph of the 80(Zn-5Al)-20Sn solder.

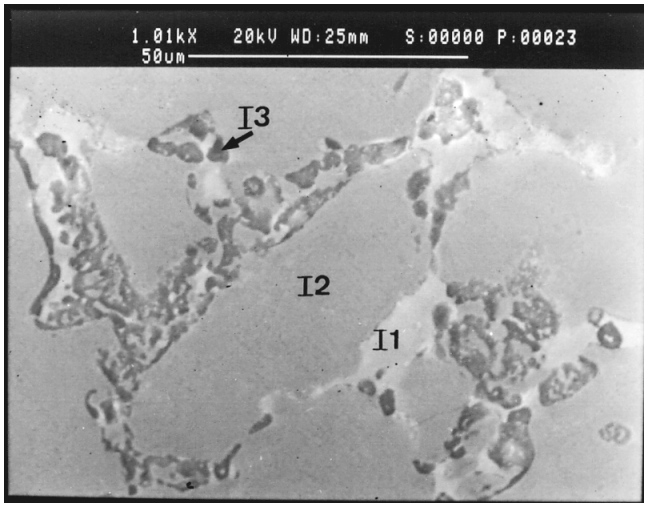

Fig. 23. The SEM micrograph of the 90(Zn-5Al)-10Sn solder.

contents are far more than that of the die casting alloys. For instance, the die casting alloy AC41A contains a maximum amount of 0.003%Sn.[19] Accordingly, the Sn of the alloys investigated in this present work actually form particular phases as described in the above discussions instead of segregating at the grain boundary as commonly encountered for the die casting alloys.

Design of the Sn-Zn-Al Solder Alloys

On the basis of the above microstructure investigation, it is apparent that the Al contents of the matrix fall in the range of 0.3%~0.9% regardless of the quantity of initial addition. The excess Al segregates to the various precipitates. Further investigations on the mechanical properties of these solder alloys and their precipitates is needed. The wetting, corrosion, and oxidation behaviors of these alloys under the conditions simulating the environments of processing or application are also needed. This work is underway. In view of the fact that the matrix can only contain a limited extent of Al, it is recommended that the Al content be less than 1%. It is easy to keep the melting point of the solder alloy of this Al composition close to the eutectic temperature. From a processing point of view, provided that the Al content is able to uniformly distribute throughout the liquid solder, the Sn-Zn-Al eutectic solder may be applied for solder processing with a wave soldering operation. However, Al may oxidize during the wave soldering process. An investigation on the liquid phase oxidation behavior of the Sn-Zn-Al solder is of importance, and is under study.

CONCLUSIONS

The eutectic reaction of the Sn-Zn-Al system occurs at 199°C. The 91Sn-8.55-Zn-0.45AI solder exhibits the eutectic behavior during cooling. A "star" precipitate with the composition of 39.2Zn-35.1Al-25.7Sn (Al_6Zn_3Sn) forms in this eutectic solder. The primary phase of the eutectic structure was found to be Sn-(5.41~12.0)Al-(3.19~5.77)Zn, while the secondary phase is Sn-1.36Zn-0.33Al. An increase in the Al and Zn contents of the Sn-Zn-Al solders complicates the cooling behaviors and the microstructures of the Sn-Zn-Al solders.

ACKNOWLEDGMENTS

The financial support of this work from the National Science Council of the Republic of China under NSC85-2216-E-006-031 is gratefully acknowledged.

REFERENCES

1. P.T. Vianco and D.R. Frear, *JOM* 45 (7), 14 (1993).
2. J.W. Morris, Jr., J.L. Freer Goldstein and Z. Mei, *JOM* 45 (7), 25 (1993).
3. C.H. Raeder, L.E. Felton, V.A. Tanzi and D.B. Knorr, *J. Electron. Mater.* 23, (7), 611 (1994).
4. L.E. Felton, C.H. Raeder and D.B. Knorr, *JOM* 45 (7), 28 (1993).
5. W.L. Winterbottom, *JOM* 45 (7), 20 (1993).
6. W. J. Tomlinson and I. Collier, *J. Mater. Sci.* 22, 1835 (1987).
7. M. Harada and R. Satoh, *IEEE Trans. Components, Hybrids, and Manufacturing Technology,* 13 (4), 736 (1990).
8. Z. Mei and J.W. Morris, Jr., *J. Electron. Mater.* 21, (6), (1992).
9. M. McCormack, S. Jin, G.W. Kammlott and H.S. Chen, *Appl. Phys. Lett.* 63, (1), 5 July, 15 (1993).
10. M. McCormack, S. Jin, H.S. Chen and D.A. Machusak, *J. Electron. Mater.* 23, (7), 687 (1994).
11. M. McCormack and S. Jin, *J. Electron. Mater.* 23 (7), 635 (1994).
12. D.B. Masson and B.K. Kirkpatrick *J. Electron. Mater.* 15, (6), 349 (1986).
13. G. Ghosh, M. Loomans and M.E. Fine, *J. Electon. Mater.* 23 (7), 619 (1994).
14. U.R. Kattner and W.J. Boettinger, *J. Electron. Mater.* 23, (7), 603 (1994).
15. C.M. Miller, I.E. Anderson and J.F. Smith, *J. Electron. Mater.* 23, (7), 595 (1994).
16. A. Sebaoun, D. Vincent and D. Treheux, *Mater. Sci. and Techn.* 3, (4), 241 (1987).
17. Z. Mei, *J. Electron. Packg. Trans. ASME* 117, (2), June, 105 (1995).
18. T.B. Massalski, *Binary Alloy Phase Diagram*, (Metals Park, OH: ASM International, 1986).
19. *Metals Handbook,* 9th Ed., Vol. 2, eds., H. Baker, D. Benjamin, C.W. Kirkpatrick, (Metals Park, OH: ASM International, 1979), p. 629.